Regular Article

PHYSICAL CHEMISTRY RESEARCH
Published by the
Iranian Chemical Society
www.physchemres.org
info@physchemres.org

***Phys. Chem. Res.**, Vol. 4, No. 1, 95-107, March 2016.*
DOI: 10.22036/pcr.2016.12401

DFT-PBE, DFT-D, and MP2 Studies on the $H_2O\cdots HNH$ and $HOH\cdots NH_2$ Hydrogen Bonds in Water-Aniline Complexes

R. Behjatmanesh-Ardakani
Department of Chemistry, Payame Noor University, P. O. Box: 19395-3697 Tehran, Iran
(Received 14 November 2015, Accepted 31 December 2015)

DFT-GGA method of Perdew-Burke-Ernzerhof (PBE) is used with aug-cc-PVTZ, 6-311++G**, and Def2-TZVP large basis sets to study the hydrogen bond interactions between oxygen lone pair as a donor electron with hydrogen atom connected to the aniline's nitrogen as an electron acceptor ($H_2O\cdots HNH$-Ph), and nitrogen lone pair with hydrogen of water molecule (Ph-$H_2N\cdots HOH$), both in the gas phase. In some cases, MP2/Def2-TZVP is also carried out to test the results of DFT. To analyze donor-acceptor interactions of two above hydrogen bonds, natural bond orbital (NBO), natural energy decomposition analysis (NEDA), natural population analysis (NPA), and quantum theory of atoms in molecules (QTAIM) methods have been used in a detailed manner. Results show that the hydrogen bond in $PhH_2N\cdots HOH$ is partially covalent, while hydrogen bond in $PhHNH\cdots OH_2$ is totally electrostatic. For the $PhHNH\cdots OH_2$ complex, there is a large gap between MP2 and PBE results which can be filled by incorporating dispersion terms in the DFT calculations. In all calculations, nitrogen atom of aniline is an stronger electron donor than the oxygen atom of water in the gas phase. $PhH_2N\cdots HOH$ has higher electron density than $PhHNH\cdots OH_2$. NBO data shows that the stabilization energy due to the charge transfer for $HOH\cdots NH_2Ph$ complex is more than that in $H_2O\cdots HNHPh$ complex. The inversion barrier energy was also calculated at the level of PBE/Def2-TZVP without and with dispersion term, and results show that the barrier energy for $PhH_2N\cdots HOH$ and $PhHNH\cdots OH_2$ complexes, are about 104 and 103 kcal mol^{-1}, without, and 8.14 and 7.03 kcal mol^{-1}, with dispersion, respectively.

Keywords: Hydrogen bond, NEDA, QTAIM, NBO, Aniline-water complex

INTRODUCTION

Aromatic compounds and their interactions with water molecules have received much attention in the literature due to the importance of water as a green solvent. Among the various studies, some researchers have focused on the gas-phase complexation of water with organic compounds. If the organic compound contains hydrogen atom connected to the electronegative atom, two kinds of interactions can be occurred. In the first cluster structure, oxygen of water interacts with the hydrogen of the organic compound, and water plays as a role of a base. In the second structure, the electronegative atom of the organic compound interacts with the hydrogen of water, and water is acid in this case. Interactions of phenol [1], anisole [2] and adenine [3], for example, with water can be classified in this field. In most cases, the cluster with water as a base ($H_2O\cdots H$-XR, X is electronegative atom and R is aromatic compound) is more stable than the other forms ($HOH\cdots X$-HR).

In the experimental studies of water-aromatic compound clusters, the role of water is characterized by comparing the electronic transition of cluster to the electronic transition of pure aromatic compound. If the water acts as a base, the red shift is observed in the electronic transition of cluster compared to its monomer. The water molecule as a base, denotes electrons to the aromatic compound, and increases the inductive effect of electronegative atom in the aromatic compound on the electronic transition; therefore, reduces frequencies of the electronic transition of complex compared to that of the organic compound without water

*Corresponding author. E-mail: behjatmanesh@pnu.ac.ir

[1a]. This kind of behavior has been observed in the case of phenol$(H_2O)_1$ compared to phenol$(H_2O)_2$ [1a]. On the other hand, compounds such as anisole (phenol with OCH_3 group instead of OH) which do not have hydrogen atom connected to the electronegative atom, can only form clusters with water molecule as an acid. In this case, blue shifting in the electronic transition of cluster is occurred compared to the pure anisole [2].

One of the aromatic compounds that its cluster formation with water is very important, is aniline. Aniline-water cluster can be formed through both mechanisms mentioned above; *i.e.*, water acts as an acid or a base. Aniline is a toxic water pollutant, and even at low concentration is harmful for aquatic life [4]. Therefore, understanding the nature of its interaction with water is important from both theoretical and experimental points of view. The first experimental study on the details of the gas-phase structure of aniline has been conducted by Lister *et al.*, Brand *et al.*, and Quack *et al.*, who studied structure and dipole moment of aniline by microwave, vibrational and fluorescence spectroscopies [5]. Kleibömer and Sutter have used combined microwave Fourier-transform with semi-rigid Bender calculation to investigate ^{14}N quadrupole hyperfine splitting of the rotational transitions of aniline in the two lowest states of the inversion motion [6]. Kerstel *et al*. studied the behavior of aniline in its first excited state using microwave-UV double resonance spectroscopy [7]. Cluster of aniline-water has been also studied experimentally and theoretically. Nakanaga and co-workers used infrared-depletion spectroscopy to specify vibrational frequencies of aniline-water cation complex [8]. Spoerel and Stahl studied hydrogen bond in the complex of aniline-water by using pulsed molecular beam Fourier-transform microwave spectroscopy [9]. Inokuchi and co-workers used DFT method to interpret measured infrared photodissociation spectra of [aniline-$(H_2O)_n]^+$, n = 1-8 [10]. Experimental and theoretical studies on the electronic transition of aniline-water complex have been investigated by Piani *et al.* [11].

In this paper, we used different quantum-chemical codes and different levels of theory to study charge transfer phenomena in the aniline-water complex. We compare our calculated results in the framework of PBE-DFT, DFT-D, and MP2 theories to the above experimental and theoretical works. The paper focuses on the properties of HOH···NH_2Ph and H_2O···HNHPh hydrogen bonds, and the energy barrier between them by locating transition state and calculating intrinsic reaction coordinates (IRC) between HOH···NH_2Ph and H_2O···HNHPh complexes.

COMPUTATIONAL DETAILS

Geometry optimization and frequency calculations were carried out with PBE [12], RIMP2 [13] and MP2 [14] levels of theory. Def2-TZVP [15], aug-cc-pVTZ [16], and 6-311++G** [17] large basis sets were used to model the wave functions. All local minima in the potential energy surface were guaranteed to be real by calculating the frequencies of normal modes which were all positive. The transition state structure had one negative/imaginary frequency in the direction of the reaction path. Spin-unpolarized calculations were considered for all monomers and complexes. Natural bond orbital and natural population analyses were carried out with the NBO6 code [18], and quantum theory of atoms in molecules (QTAIM) calculations were carried out with the AIM2000 [19] program. GAMESS-US [20] program was employed for all PBE/aug-ccpVTZ calculations. All other calculations (including PBE/Def2-TZVP, RI-MP2/Def2-TZVP, and PBE/6-311++G**) were carried out by the ORCA code [21]. To do NBO6 calculations, its binary files were linked to the GAMESS-US and ORCA programs. Graphical shapes of the natural bond orbital interactions were generated by JmolNBO [22] program. For DFT-D calculations in ORCA code, the model of D3(BJ) dispersion [23] was chosen to add the dispersion term in the standard DFT. Equation of D3(BJ) dispersion term is:

$$E_{disp}^{D3(BJ)} = -\frac{1}{2}\sum_{A\neq B} s_6 \frac{C_6^{AB}}{R_{AB}^6 + \left[f\left(R_{AB}^0\right)\right]^6} + s_8 \frac{C_8^{AB}}{R_{AB}^8 + \left[f\left(R_{AB}^0\right)\right]^8} \quad (1)$$

with $f\left(R_{AB}^0\right) = a_1 R_{AB}^0 + a_2$.

S_6 = 1.0, a_1 = 0.4289, s_8 = 0.7879, and a_2 = 4.4407 were chosen for dispersion calculations. All DFT-D parameters and model in the GAMESS-US code were taken from Peverati and Baldridge [24].

RESULTS AND DISCUSSION

Geometric Structures

Figure 1 shows the optimized structure of aniline in the level of MP2/Def2-TZVP. The most important structural parameter in aniline is the angle between NH_2 and plane of the benzene ring. Different authors with different experimental techniques tried to measure it; however, due to the crude approximations on which their calculations were based, several degree of differences have been reported. Lister *et al*. have reported that the out-of-plane angle of the NH_2 group is 37˚ 29′ [5b]. Kleibömer and Sutter have reported the torsion angle of 44˚ 18′ between NH_2 and ring planes [6]. Brand and co-workers reported 45˚ for the out-of-plane angle of NH_2 in aniline ring [5c,25]. Our calculated out-of-plane angles of NH_2 in pure aniline are 39˚ 41′, 40˚ 5′, and 44˚ 52′ for PBE/aug-cc-pVTZ, PBE-Def2-TZVP, and MP2/Def2-TZVP, respectively, which are in good agreement with the experimental data. The other important structural-physical parameter is dipole moment, which can be easily calculated from microwave spectroscopy. Lister *et al*. have reported dipole moment of 1.129D for aniline molecule in the gas phase [5b]. Our calculated dipole moments of aniline are 1.691D, 1.782D, and 1.544D for PBE/aug-cc-pVTZ, PBE-Def2-TZVP, and MP2/Def2-TZVP, respectively.

Figure 2 shows the optimized structures of aniline-water clusters in the gas phase at the level of PBE/def2-TZVP. It should be noted that the optimized structures at the level of PBE/aug-ccpVTZ are similar to the structures of Fig. 2. Two structures have been considered for the aniline-water cluster. The first one contains $HOH\cdots NH_2Ph$ hydrogen bond in which water acts as an acid, and the second one contains $H_2O\cdots HNHPh$ hydrogen bond in which water molecule acts as a base. Nakanaga *et al*., using infrared-depletion spectroscopy, have shown that there is a strong hydrogen bond between lone pair of water and hydrogen of NH_2 group ($H_2O\cdots HNHPh$) in the cation-complex of aniline-water [8]. Out of the experimental frequencies, they argued that there is no hydrogen bond between lone pair of nitrogen and hydrogen of water in the cluster-cation of aniline-water. For the neutral aniline-water complex, they have reported results of theoretical calculations at MP2/6-31G**. Based on their theoretical

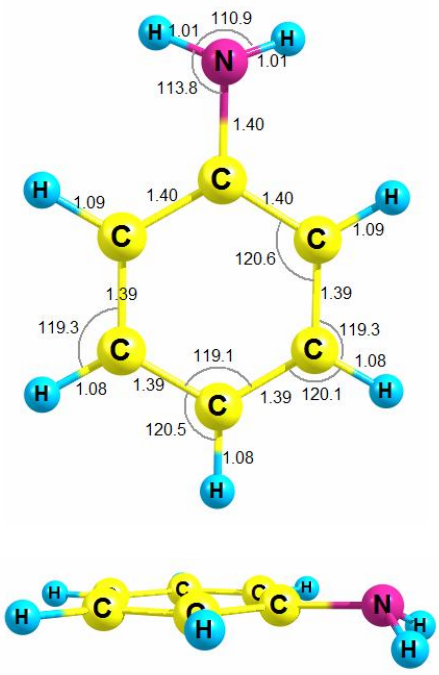

Fig. 1. Optimized structure of aniline from top and side views, calculated at MP2/Def2-TZVP by ORCA program.

results, $HOH\cdots NH_2Ph$ has stronger hydrogen bond than that in the interaction of $H_2O\cdots H_2NPh$ (D_e of 2390 cm^{-1} *vs*. 2290 cm^{-1}). In summary, Nakanaga *et al*. found that for the case of cation-complex, $H_2O\cdots H_2NPh$ has stronger hydrogen bond, while for the neutral-complex case, $HOH\cdots NH_2Ph$ is more stable than the other complex. Our binding energies (see the next section) confirm the Nakanaga results for the neutral complex.

Different attitudes of neutral and cation complexes in reactions can be described by the observed frequencies in the Nakanaga's paper [8]. Among frequencies observed for absorption bands in the Nakanaga's work, two strong bands at 3636 and 3715 cm^{-1} in the OH stretching vibration region have been assigned to the symmetric and anti-symmetric vibrations of OH bonds of H_2O in the cation-complex. These frequencies are only 20 and 42 cm^{-1} less than those of the symmetric and anti-symmetric stretching vibrations of the neutral H_2O, So, H_2O in the cation-complex is neutral, and the HOMO in the cation-complex system belongs to the aniline molecule (the OH stretching frequency of H_2O^+ is as

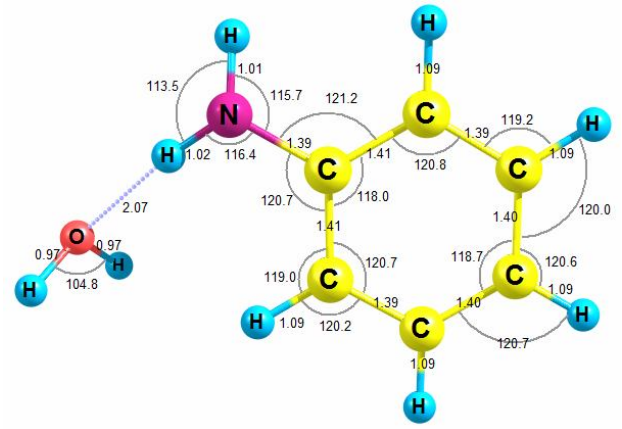

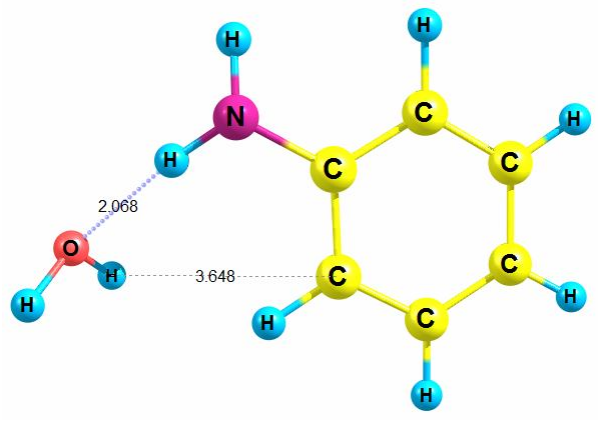

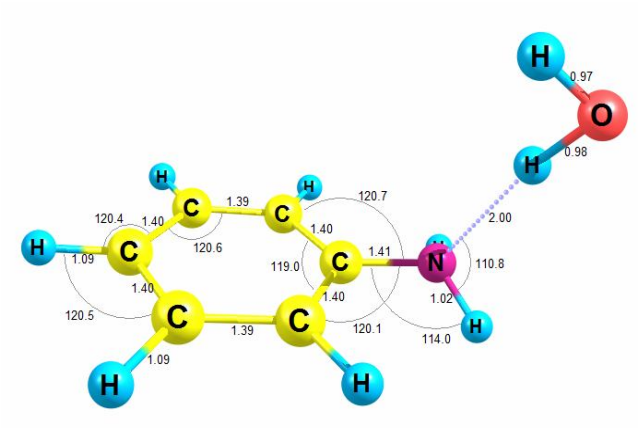

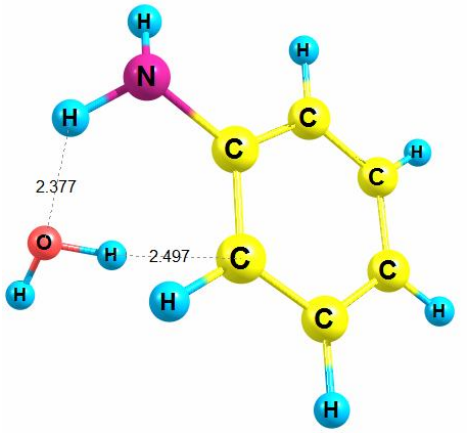

Fig. 2. Optimized structures of $H_2O\cdots HNHPh$ (left) and $HOH\cdots NH_2Ph$ (right) complexes calculated at PBE/Def2-TZVP by ORCA program.

Fig. 3. Optimized structures of $H_2O\cdots HNHPh$ at the levels of PBE/Def2-TZVP and MP2/Def2-TZVP from similar starting configurations calculated by ORCA program.

low as 3200 cm^{-1}). To compensate its charge reduction, aniline tends to interact with oxygen of water and acts as an acid. Therefore, for the cation-complex, the $H_2O\cdots H_2NPh$ complex has the stronger hydrogen bond than the $HOH\cdots NH_2Ph$ complex. On the other hand, for the neutral complex, there is no any charge reduction in the aniline, and it can acts as a base; so, in the neutral case $HOH\cdots NH_2Ph$ is more stable than the other complex.

It is interesting to compare vibrational frequencies of OH stretching region in our calculated neutral complexes with the cation-complex of Nakanaga's paper. If our discussion on the presence of HOMO on aniline is correct, then the difference between our calculated OH stretching frequencies of neutral complex in the form of aniline, as a base (HOMO on aniline), with the calculated data for cation-complex should be low. Nakanaga's calculated frequencies for OH anti-symmetric and symmetric stretching are 3636 and 3715 cm^{-1}, respectively. Calculated frequencies for the OH stretching mentioned in this work, at the level of MP2/Def2-TZVP, are 3678 and 3883 cm^{-1}, respectively, for $HOH\cdots NH_2Ph$ complex, and 3770 and 3907 cm^{-1}, respectively, for $H_2O\cdots H_2NPh$. Comparing calculated frequencies show that frequencies of the OH stretching for $HOH\cdots NH_2Ph$ complex are close to the experimental data. It shows that the Nakanaga's argument for assuming HOMO on aniline is correct.

Figure 3 shows the neutral cluster of aniline and water

molecule in which water functions as an acid, at two levels PBE/Def2-TZVP and MP2/Def2-TZVP. As clearly seen in Fig. 3, optimized clusters at two theoretical levels, PBE and MP2, do not show the same structural features. In PBE-DFT optimized structure, the hydrogens of water molecule do not interact with the aromatic ring, and are directed away from the aromatic ring; however, for MP2 optimized structure, one of the hydrogens is oriented towards C3 of the aromatic ring (in the next sections, we will show that there is a bond critical point between these two atoms).

DFT methods suffer from the lack of dispersion in their equations. It is worth trying the addition of dispersion term in the PBE-DFT method (DFT-D) can fill the gap between MP2 and DFT or not. Figure 4 shows the optimized structure of initial configuration of Fig. 3 using DFT-D method. As clearly seen, the H atom of water molecule interacts with C3 of the benzene ring exactly similar to the MP2 optimized structure. O···H distance increases from 2.07 (for DFT) to 2.23A (for DFT-D) which is more close to the MP2 distance (2.38A). The geometrical data shows that the dispersion introduction to the DFT equations can fill the gap between DFT and MP2 in the case of studied complex.

The out-of-plane angle of NH_2 group in aniline in the cluster form is different from that in the pure aniline. This angle is 47˚ 54′ for MP2/Def2-TZVP, when the water is base (for $H_2O\cdots HNHPh$ interaction), and is 46˚ 45′ for MP2/Def2-TZVP, when the water is acid (for $HOH\cdots NH_2Ph$ interaction). Comparing the data with the out-of-plane angle of NH_2 in pure aniline clearly shows that for both hydrogen bond interactions, the angle has been increased. Using pulsed molecular beam Fourier-transform microwave spectroscopy, Spoerel and Stahl showed that in $HOH\cdots NH_2Ph$ type of hydrogen bond interaction, orientation of the second hydrogen of water, which does not interact with N of NH_2 group, changes towards the aromatic ring [9]. Our calculated result in Fig. 2 is exactly the same as the experimental results. We tried different initial configurations whose second hydrogen of water was directed away from the aromatic ring, but after optimization, the hydrogen rotated towards the aromatic ring.

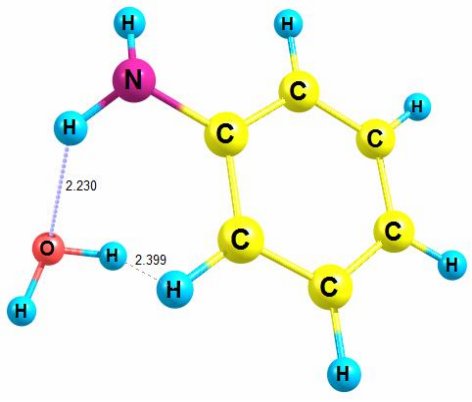

Fig. 4. Optimized structures of $H_2O\cdots HNHPh$ at the level of DFT-D (PBE-D3/Def2-TZVP) from similar starting configuration of Fig. 3 by ORCA program.

Binding Energies

Table 1 shows the electronic energies (E_{ele}), electronic energies corrected by zero-point energies (E_{ele}^{ZPE}), binding energies (ΔE_{ele}^{ZPE}), corrected binding energies ($\Delta E_{ele}^{ZPE+BSSE}$) with basis set superposition error (BSSE) by the counterpoise method of Boys and Bernardi [26], and Gibbs free energies of two clusters with different hydrogen bonds. Data shows that the corrected binding energy for $H_2O\cdots HNHPh$ is -2.06 kcal mol^{-1} and for $HOH\cdots NH_2Ph$ is -3.62 kcal mol^{-1} at MP2/Def2-TZVP in the gas phase. In all calculations the cluster with water as an acid is more stable than the other form. The largest difference between binding energies of two forms of the clusters belong to the MP2/Def2-TZVP calculation with 1.56 kcal mol^{-1}. On the other hand, taking the dispersion term into account (DFT-D) shows that for $HOH\cdots NH_2Ph$, $H_2O\cdots HNHPh$, NH_2Ph, and H_2O, the dispersion energy is -0.0158, -0.0158, -0.0133 and -0.0004 Ha, respectively. For two studied complexes, the dispersion energy stabilization for E_{ele} is equal to -9.91 kcal mol^{-1}. It shows that binding energies for two complexes more stabilized by 1.32 kcal mol^{-1} due to the dispersion energy.

In the optimized cluster at MP2/Def2-TZVP level, as explained in previous section, hydrogen of water molecule (as an acid) interacts simultaneously with the aromatic ring and lone pair of nitrogen. Calculated dipole moments of

Table 1. Electronic Energy (E_{ele}, in Hartree), Corrected Electronic Energy (E_{ele}^{ZPE}, in Hartree), Corrected Binding Energy ($\Delta E_{ele}^{ZPE+BSSE}$, in Hartree), and Gibbs Free Energy (in Hartree) of the Studied Species. All Data were Rounded to Five Decimal Places

	Compound	E_{ele}	E_{ele}^{ZPE} [1]	$\Delta E_{ele}^{ZPE+BSSE}$	G[1]
PBE/aug-cc-pVTZ	Aniline	-287.33995	-287.22626	-	-287.25550
	Water	-76.38052	-76.35982	-	-76.37749
	HNH···OH_2	-363.72649	-363.59050	-0.00432	-363.62554
	H_2N···HOH	-363.72890	-363.59180	-0.00562	-363.62394
PBE/Def2-TZVP	Aniline	-287.34114	-287.22763	-	-287.25689
	Water	-76.37691	-76.35624	-	-76.37391
	HNH···OH_2	-363.72615	-363.58989	-0.00443	-363.62395
	H_2N···HOH	-363.72772	-363.59075	-0.00500	-363.62261
RI-MP2/Def2-TZVP	Aniline	-286.97785	-286.86109	-	-286.89031
	Water	-76.31313	-76.29178	-	-76.30941
	HNH···OH_2	-363.29954	-363.15923	-0.00419	-363.19272
	H_2N···HOH	-363.30196	-363.16086	-0.00490	-363.19385
MP2/Def2-TZVP	Aniline	-286.97779	-286.86104	-	-286.89026
	Water	-76.31306	-76.29169	-	-76.30933
	HNH···OH_2	-363.29951	-363.15913	-0.00328	-363.19251
	H_2N···HOH	-363.30183	-363.16067	-0.00577	-363.19369

[1]Corrected for the symmetry numbers in calculation rotational entropy. [2]Symmetry number of water is 2, for others are 1, even for aniline.

$H_2O\cdots HNHPh$ and $HOH\cdots NH_2Ph$ complexes, at the level of MP2/Def2-TZVP, are 1.8 and 3.3 Debye, respectively. HOMO and LUMO energies of $H_2O\cdots HNHPh$ and $HOH\cdots NH_2Ph$ are -0.1688, -0.0307, -0.1999 and -0.0484 Hartree, respectively. Available results show that both HOMO and LUMO of $HOH\cdots NH_2Ph$ complex are more stable than those of the $H_2O\cdots HNHPh$ complex. Relaxed MP2 Mulliken charge density shows that the charge on nitrogen atom in the $H_2O\cdots HNHPh$ complex is -0.48, while it is -0.52 for $HOH\cdots NH_2Ph$ complex. Other atoms have nearly the same relaxed MP2 Mulliken charge density for both clusters.

It is possible to calculate transition state structure (TS) between two conformations of aniline-water complexes. At the first step, transition state location is searched in the potential energy surface, and then the structure is optimized. Normal mode calculations on the TS showed that the 6^{th} mode is imaginary. Potential energy surface scan along the imaginary normal mode proved that the calculated TS belongs to the $H_2O\cdots HNHPh$ and $HOH\cdots NH_2Ph$ complexes. Figure 5 shows barrier energy of TS relative to the optimized energies of complexes. The barrier energies for $H_2O\cdots HNHPh$ and $HOH\cdots NH_2Ph$ complexes at the PBE/Def2-TZVP level of theory are 103.21 and 104.19 kcal mol^{-1}, respectively. Introducing dispersion correction terms to calculations reduces barrier energies of $H_2O\cdots HNHPh$ and $HOH\cdots NH_2Ph$ complexes to 7.03 and 8.14 kcal mol^{-1}, respectively. Based on our results, transformation of complexes to each other at the room temperature is not possible. .

NBO and AIM Analyses

Natural bond orbital (NBO) translates mathematical language of quantum chemistry to the well-known concepts in chemistry such as hybridization, conjugation, hyper-conjugation, charge transfer, and orbital interactions. Lewis orbitals in NBO are “core” and “bonding” orbitals which are highly occupied, and non-Lewis orbitals are “anti-bonds” and “Rydberg” orbitals with low occupation number [27]. In the NBO framework, stabilization energy due to the charge

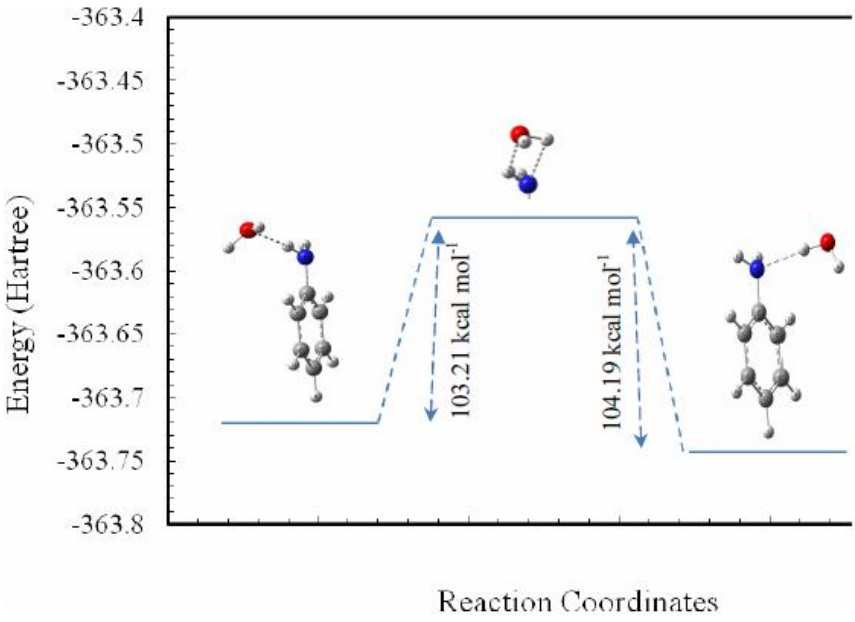

Fig. 5. Barrier energy of transition state (TS) for two studied complexes. For N···H and O···H complexes, barrier energies are 104.19 and 103.21 kcal mol^{-1}, respectively. Introducing dispersion term in DFT, reduces the barrier energies to 8.14 and 7.03 kcal mol^{-1}, respectively.

transfer between a donor (i) and acceptor (j) is estimated by the following equation [27]:

$$E^{(2)} = \Delta E_{i\rightarrow j} = q_i \frac{F^{(2)}(i,j)}{\varepsilon_j - \varepsilon_i} \quad (2)$$

where, $E^{(2)}$ is stabilization energy, q_i is occupation number of donor orbital, ε_j and ε_i are orbital energies, and $F^{(2)}$ are off-diagonal element of NBO Fock matrix.

Table 2 shows stabilization energy, hybridization, and occupation numbers of donor and acceptor orbitals for hydrogen bonds in $H_2O\cdots HNHPh$ and $HOH\cdots NH_2Ph$ complexes at the level of PBE/Def2-TZVP. Both Def2-TZVP and aug-cc-pVTZ basis sets predict that the $E^{(2)}$ of hydrogen bond in the $HOH\cdots NH_2Ph$ complex is higher than that of hydrogen bond in $H_2O\cdots HNHPh$ complex.

Hybridization of lone pair of nitrogen in $H_2O\cdots HNHPh$ is $sp^{8.35}d^{0.01}$ (%p = 89%), while for $HOH\cdots NH_2Ph$ is $sp^{5.42}$ (%p = 84%) indicative of more contribution of this lone pair, in the first complex, in the conjugation process of the ring compared to that in the second complex. Higher %p in hybridization of LP of N1 in Table 2 compared to that in hybridization of O15 LP is also a result of the ring conjugation with LP(1)N1. The stabilization energy of charge transfer from LP(1)N1 to the first unoccupied orbital of C2 atom (LV(1)C2) in $H_2O\cdots HNHPh$ is 89.49 kcal mol^{-1}, while for $HOH\cdots NH_2Ph$ is 63.24 kcal mol^{-1}. This is also a result of interaction of LP(1)N1 with hydrogen of water molecule in the $HOH\cdots NH_2Ph$ complex which prevent LP(1)N1 to be completely introduced in the conjugation process. Figure 6 shows three dimensional donor-acceptor orbital interactions of hydrogen bonds in $H_2O\cdots HNHPh$ and $HOH\cdots NH_2Ph$ complexes. As the pictures clearly show, there is a good overlap between donor and acceptor orbitals in both complexes.

Natural energy decomposition analysis (NEDA) help us to understand the nature of interactions in terms of meaningful physical components [28]. NEDA decomposes molecular interaction energy to the charge transfer (CT), electrostatic (ES), polarization (POL), Pauli exchange (EX) and core repulsion or deformation (DEF) contributions. Deformation component of energy has always a positive value, and therefore it is a destabilizing quantity. The POL component arises from induced electrical interactions between two fragments. The difference between $\Delta E_{binding}^{BSSE}$ and ΔE_{NEDA} (which is the sum of CT+POL+ES+XC+DEF) is known as the distortion energy, defined as the energy required for changing the optimized structures of the ligands in their isolated forms to their structures in the complex.

For $H_2O\cdots HNHPh$ complex, CT, ES, POL and XC components are -106.16, -5.77, -6.76 and +86.99 kcal mol^{-1}, respectively, while for $HOH\cdots NH_2Ph$ complex, they are -151.05, -9.85, -3.03 and +125.59 kcal mol^{-1}, respectively. Both NEDA calculations are at DFT-D (PBE/aug-cc-pVTZ with dispersion) by GAMESS-US code. Data show that for both complexes CT >> ES. It has been previously shown

Table 2. NBO6 Data for Hydrogen Bonds in Two Complexes. Data Calculated at the Level of PBE/Def2-TZVP by ORCA Program. $E^{(2)}$ Values are in kcal mol^{-1}

Complex	Donor	Acceptor	Occ[a]	$E^{(2)b}$
$PhHNH\ldots OH_2$	LP(1) O15 [$sp^{2.27}$]	BD*(1) N1-H8 [$sp^{2.62}d^{0.0}$]	1.996(0.021)	0.15(0.15)
	LP(2) O15 [$sp^{3.18}$]	BD*(1) N1-H8 [$sp^{2.62}d^{0.0}$]	1.983(0.021)	5.17(0.84)
$PhH_2N\ldots HOH$	LP(1) N1 [$sp^{5.42}$]	BD*(1) O15-H17 [$sp^{2.98}d^{0.01}$]	1.840(0.026)	9.08(11.6)

[a]Occupation number. Data in parentheses are for acceptor orbitals. [b]Data in parentheses belong to DFT-D (PBE/aug-cc-pVTZ+dispersion) calculated with GAMESS-US code.

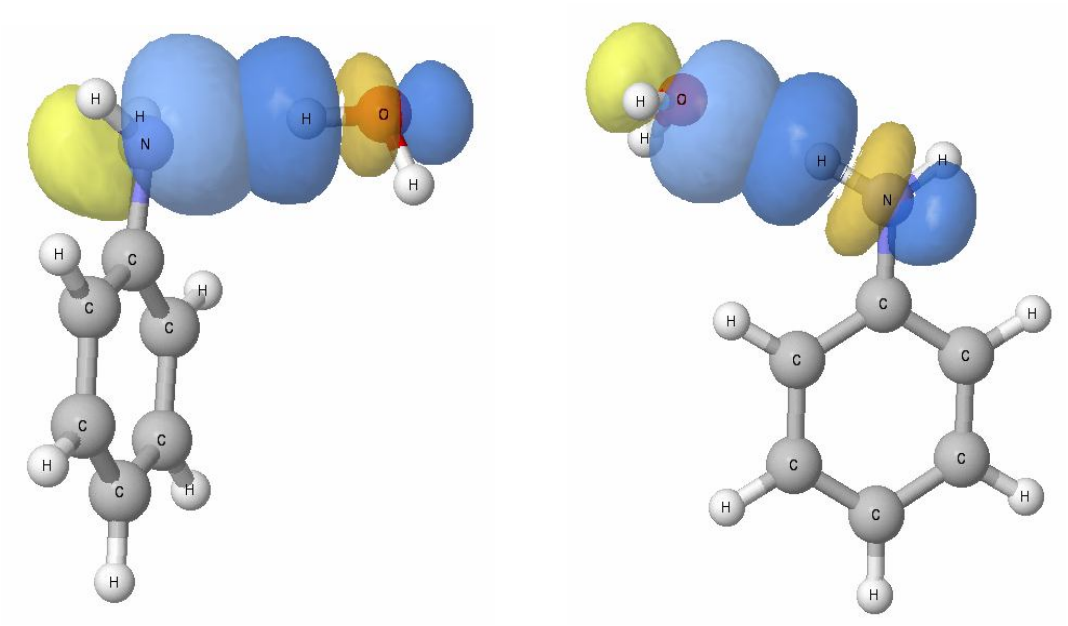

Fig. 6. Donor-Acceptor orbital interactions in $HOH\cdots NH_2Ph$ (left) and $H_2O\cdots HNHPh$ (right) complexes. Both calculations have been carried out at PBE/Def2-TZVP by ORCA program.

Table 3. NBO, QTAIM and Mulliken Charges for some Important Atoms in the Complexes

Complex	Atom	NBO[1]	AIM[b]	Mulliken[a]
$PhHNH\ldots OH_2$	N1	-0.77(-0.80)	-1.026	-0.41(-0.55)
	H8	0.41(0.40)	0.42	0.25(0.10)
	H9	0.37(0.38)	0.36	0.22(0.09)
	O15	-0.93(-0.94)	-1.06	-0.62(-0.39)
	H16	0.47(0.47)	0.55	0.33(0.12)
	H17	0.47(0.47)	0.55	0.33(0.24)
$PhH_2N\ldots HOH$	N1	-0.79(-0.79)	-0.98	-0.45(-0.36)
	H8	0.38(0.39)	0.37	0.23(0.02)
	H9	0.39(0.39)	0.37	0.25(0.00)
	O15	-0.95(-0.95)	-1.09	-0.63(-0.44)
	H16	0.45(0.46)	0.52	0.30(0.13)
	H17	0.47(0.47)	0.55	0.32(0.29)

[a]Data in parentheses belong to DFT-D (PBE/Aug-cc-pVTZ+dispersion) calculated by. [b]Wavefunctions have been calculated at PBE/6-311++G** by ORCA program.

that ES has a nature of long-range, and CT is short-range [28b]. Covalent character of an intermolecular bond is calculated by CT/(CT+ES), which CT is associated with covalent delocalization, and ES with ionic interactions. This ratio is 94.8% for $H_2O\cdots HNHPh$ complex, and 93.9% for $HOH\cdots NH_2Ph$ complex. NEDA data show that both hydrogen bonds in complexes are partially covalent.

Quantum theory of atoms in molecules (QTAIM) is a good method to analyze the intermolecular interactions [29]. In QTAIM, a bond between two atoms is characterized by the presence of a bond path between them. A bond path contains bond critical point for which gradient of electron density is zero. Electron density value at bond critical point (ρ_b) is a measure of bond strength.

For the shared shell interactions, such as covalent bonds, ρ_b is of the order of 0.1, while for the closed shell interactions, such as hydrogen bonds, it is in the order of 0.01 $eÅ^{-3}$. Total energy, shown by H, is also an important parameter in classification of intermolecular interactions. For covalent bonds, H is a high negative value. For partially covalent interaction, H is negative, but near to zero. For shared-shell interactions such as covalent bonds, laplacian is always negative and high, but for closed-shell interactions it is low and positive.

Electron density, laplacian, and total energy for the bond critical point in $H_2O\cdots HNHPh$ complex are 0.02, 0.073 and 0.003 (in atomic unit), respectively, and for $HOH\cdots NH_2Ph$ complex, are 0.029, 0.079 and -0.001. Data show that the hydrogen bond in $H_2O\cdots HNHPh$ complex is electrostatic, while for $HOH\cdots NH_2Ph$ is partially-covalent partially electrostatic. This result is in line with the NBO data which predict charge transfer in $HOH\cdots NH_2Ph$ is stronger than that in $H_2O\cdots HNHPh$.

Table 3 shows NBO, QTAIM, and Mulliken charges on the important atoms in both $H_2O\cdots HNHPh$ and $HOH\cdots NH_2Ph$ complexes. For $H_2O\cdots HNHPh$ complex in which lone pair of oxygen is electron donor, it is expected that its charge to be less than the oxygen charge in $HOH\cdots NH_2Ph$. On the other hand, nitrogen charge in $H_2O\cdots HNHPh$ complex is expected to be less than that in $HOH\cdots NH_2Ph$ complex. Comparing three different charge calculation algorithms in Table 3 shows that the QTAIM charges are more reliable than the NBO and Mulliken charges. It is worth noting that the hydrogen atom which

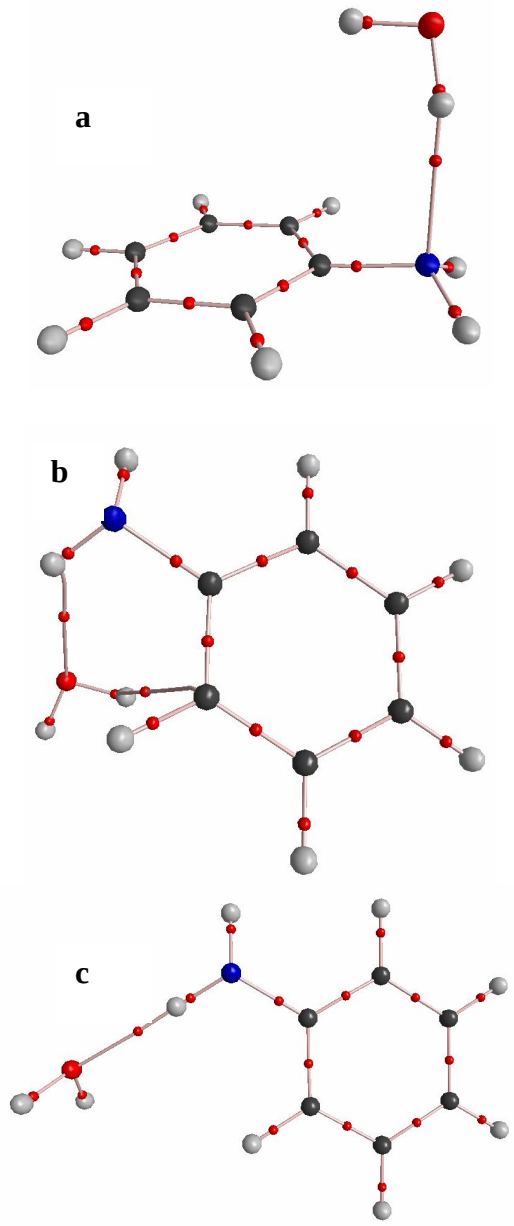

Fig. 7. Molecular graphs of $HOH\cdots NH_2Ph$ (a) and $H_2O\cdots HNHPh$ (b, c) complexes. Hydrogen, carbon, oxygen, and nitrogen atoms are shown in gray, black, red and blue, respectively. Two above graphs (a, b) hane been preparedat MP2/ Def2-TZVP, and the third one (c) at PBE/Def2-TZVP. All calculations have been carried out by ORCA/AIM2000 programs. Addition of dispersion term to DFT, changes the molecular graph from "c" to "b".

form hydrogen bond is more positive compared to the other hydrogen atom. This can be explained by the induction effect of electronegative atom connected to it. Figure 7 shows the molecular graphs of two studied complexes. In molecular graph of $H_2O\cdots HNHPh$ complex optimized with MP2 (structure b), there are two critical points between water and aniline molecules. The first one belongs to $O\cdots NH$, and the second one belongs to $H\cdots C3$, while for PBE (structure c), there is only one critical point belonging to $O\cdots NH$.

CONCLUSIONS

In this paper, interactions of $H_2O\cdots HNHPh$ and $HOH\cdots NH_2Ph$ complexes have been analyzed by the modern algorithms of NBO, NPA, NEDA and QTAIM. Binding energy calculations show that $HOH\cdots NH_2Ph$ complex is more stable than $H_2O\cdots HNHPh$. At the level of MP2/Def2-TZVP it is more stable about 1.5 kcal mol^{-1} which is higher than the kinetic energy of molecules in room temperature. Its dipole moment is nearly two times more than that of $H_2O\cdots HNHPh$, and its HOMO and LUMO are more stable than those of $H_2O\cdots HNHPh$. Transition state energy calculation, without dispersion term, shows that the activation energy of the forward reaction ($HOH\cdots NH_2Ph$ complex to the TS) is about 104 kcal mol^{-1} and the activation energy of the reverse reaction ($H_2O\cdots HNHPh$ complex to TS) is about 103 kcal mol^{-1}. Taking into account the term of dispersion in DFT, the activation energies redice to 8.1 and 7.0 kcal mol^{-1}, respectively. NBO data show that the stabilization energy due to the charge transfer for $HOH\cdots NH_2Ph$ complex is more than that in $H_2O\cdots HNHPh$ complex. NEDA results show that the most important part in hydrogen bond interactions of both complexes is charge transfer. QTAIM results also confirm the NEDA data. Comparing the charges show that the QTAIM algorithm presents better results than the NBO or Mulliken methods.

ACKNOWLEDGEMENTS

I would like to thank Payame Noor University (PNU) for the support of this work.

REFERENCES

[1] a)Berden, G.; Meerts, W. L.; Schmitt, M.; Kleinermanns, K., High resolution UV spectroscopy of phenol and the hydrogen bonded phenol-water cluster. *J. Chem. Phys.*, **1996**, *104*, 972-982, DOI:10.1063/1.470821; b) Parthasarathi, R.; Subramanian, V.; Sathyamurthy, N., Hydrogen bonding in phenol, water, and phenol-water clusters. *J. Phys. Chem. A*, **2005**, *109*, 843-850, DOI: 10.1021/jp046499r.

[2] a) Becucci, M.; Pietraperzia, G.; Pasquini, M.; Piani, G.; Zoppi, A.; Chelli, R.; Castellucci, E.; Demtroeder, W., A study on the anisole-water complex by molecular beam-electronic spectroscopy and molecular mechanics calculations. *J. Chem. Phys.*, **2004**, *120*, 5601-5607, DOI:10.1063/1.1648635; b) Ribblett, J. W.; Sinclair, W. E.; Borst, D. R.; Yi, J. T.; Pratt, D. W., High resolution electronic spectra of anisole and anisole-water in the gas phase: hydrogen bond switching in the S1 State†. *J. Phys. Chem. A*, **2006**, *110*, 1478-1483, DOI: 10.1021/jp052832v.

[3] a) Kim, N. J.; Kang, H.; Jeong, G.; Kim, Y. S.; Lee, K. T.; Kim, S. K., Anomalous fragmentation of hydrated clusters of DNA base adenine in UV photoionization. *J. Phys. Chem. A*, **2000**, *104*, 6552-6557, DOI: 10.1021/jp000813+; b) Kang, H.; Lee, K. T.; Kim, S. K., Femtosecond real time dynamics of hydrogen bond dissociation in photoexcited adenine-water clusters. *Chem. Phys. Lett.*, **2002**, *359*, 213-219, DOI: 10.1016/S0009-2614(02)00773-X.

[4] Xiao, G.; Long, L., Efficient removal of aniline by a water-compatible microporous and mesoporous hyper-cross-linked resin and XAD-4 resin: A comparative study. *Appl. Surf. Sci.*, **2012**, *258*, 6465-6471, DOI: 10.1016/j.apsusc.2012.03.062.

[5] a)Lister, D. G.; Tyler, J. K., Non-planarity of the aniline molecule. *Chem. Commun.*, **1966**, 152-153, DOI: 10.1039/C19660000152; b) Lister, D. G.; Tyler, J. K.; Høg, J. H.; Larsen, N. W., The

microwave spectrum, structure and dipole moment of aniline. *J. Mol. Struct.,* **1974**, *23*, 253-264, DOI: 10.1016/0022-2860(74)85039-8; c) Brand, J. C. D.; Williams, D. R.; Cook, T. J., Vibrational analysis of the first ultraviolet band system of aniline. *J. Mol. Spectrosc.,* **1966**, *20*, 359-380, DOI: 10.1016/0022-2852(66)90008-7; d) Quack, M.; Stockburger, M., Resonance fluorescence of aniline vapour. *J. Mol. Spectrosc.,* **1972**, *43*, 87-116, DOI: 10.1016/0022-2852(72)90164-6.

[6] Kleibömer, B.; Sutter, D., The vibrational state dependence of the 14N quadrupole coupling tensor in aniline. A microwave Fourier-transform study combined with semirigid bender calculations. *Z. Naturforsch., A: Phys. Sci.,* **1988**, *43*, 561-571, DOI: 10.1515/zna-1988-0607.

[7] Kerstel, E. R. T.; Becucci, M.; Pietraperzia, G.; Castellucci, E., High-resolution absorption, excitation, and microwave-UV double resonance spectroscopy on a molecular beam: S1 aniline. *Chem. Phys.*, **1995**, *199*, 263-273, DOI: 10.1016/0301-0104(95)00181-M.

[8] Nakanaga, T.; Kawamata, K.; Ito, F., Infrared depletion spectroscopy of the aniline-H2O+ cluster cation. *Chem. Phys. Lett.*, **1997**, *279*, 309-314, 10.1016/S0009-2614(97)01059-2.

[9] Spoerel, U.; Stahl, W., The aniline-water complex. *J. Mol. Spectrosc.*, **1998**, *190*, 278-289, 10.1006/jmsp.1998.7600.

[10] Inokuchi, Y.; Ohashi, K.; Honkawa, Y.; Yamamoto, N.; Sekiya, H.; Nishi, N., Infrared photodissociation spectroscopy of [aniline-(water)n] + (n = 1-8): structural change from branched and cyclic to proton-Transferred Forms. *J. Phys. Chem. A*, **2003**, *107*, 4230-4237, DOI: 10.1021/jp0225525.

[11] Piani, G.; Pasquini, M.; López-Tocón, I.; Pietraperzia, G.; Becucci, M.; Castellucci, E., The aniline-water and aniline-methanol complexes in the S1 excited state. *Chem. Phys.,* **2006**, *330*, 138-145, DOI: 10.1016/j.chemphys.2006.08.004.

[12] Perdew, J. P.; Burke, K.; Ernzerhof, M., Generalized gradient approximation made simple. *Phys. Rev. Lett.,* **1996**, *77*, 3865-3868, DOI: 10.1103/PhysRevLett.78.1396.

[13] Kossmann, S.; Neese, F., Efficient structure optimization with second-order many-body perturbation theory: The RIJCOSX-MP2 Method. *J. Chem. Theory Comput.*, **2010**, *6*, 2325-2338, DOI: 10.1021/ct100199k.

[14] Sæbø, S.; Almlöf, J., Avoiding the integral storage bottleneck in LCAO calculations of electron correlation. *Chem. Phys. Lett.*, **1989**, *154*, 83-89, DOI: 10.1016/0009-2614(89)87442-1.

[15] Weigend, F.; Ahlrichs, R., Balanced basis sets of split valence, triple zeta valence and quadruple zeta valence quality for H to Rn: Design and assessment of accuracy. *Phys. Chem. Chem. Phys.*, **2005**, *7*, 3297-3305, DOI: 10.1039/B508541A.

[16] Dunning, T. H., Gaussian basis functions for use in molecular calculations. IV. The representation of polarization functions for the first row atoms and hydrogen. *J. Chem. Phys.*, **1971**, *55*, 3958-3966, DOI: 10.1063/1.1676685.

[17] Krishnan, R.; Binkley, J. S.; Seeger, R.; Pople, J. A., Self-consistent molecular orbital methods. XX. A basis set for correlated wave functions. *J. Chem. Phys.*, **1980**, *72*, 650-654, DOI: 10.1063/1.438955.

[18] Glendening, E. D.; Badenhoop, J. K.; Reed, A. E.; Carpenter, J. E.; Bohmann, J. A.; Morales, C. M.; Landis, C. R.; Weinhold, F.

[19] Biegler-König, F.; Schönbohm, J., Update of the AIM2000-Program for atoms in molecules. **2002**, *23*, 1489-1494, 10.1002/jcc.10085.

[20] Schmidt, M. W.; Baldridge, K. K.; Boatz, J. A.; Elbert, S. T.; Gordon, M. S.; Jensen, J. H.; Koseki, S.; Matsunaga, N.; Nguyen, K. A.; Su, S.; Windus, T. L.; Dupuis, M. ; Montgomery, J. A., General atomic and molecular electronic structure system. *J. Comput. Chem.*, **1993**, *14*, 1347-1363, DOI: 10.1002/jcc.540141112.

[21] Neese, F., The ORCA program system. *Wiley Interdiscip. Rev. Comput. Mol. Sci.*, **2012**, *2*, 73-78,

DOI: 10.1002/wcms.81.

[22] Jmol-NBO Visualization Helper. http://www.marcelpatek.com/nbo/nbo.html.

[23] Grimme, S.; Antony, J.; Ehrlich, S.; Krieg, H., A consistent and accurate ab initio parametrization of density functional dispersion correction (DFT-D) for the 94 elements H-Pu. **2010**, *132*, 154104, DOI: 10.1063/1.3382344.

[24] Peverati, R.; Baldridge, K. K., Implementation and performance of DFT-D with respect to basis set and functional for study of dispersion interactions in nanoscale aromatic hydrocarbons. **2008**, *4*, 2030-2048, 10.1021/ct800252z.

[25] Brand, J. C.; Williams, D. R. ; Cook, T. J., Aniline-planar or nonplanar? *J. Mol. Spectrosc.*, **1966**, *20*, 193-195, DOI: 10.1016/0022-2852(66)90055-5.

[26] Boys, S. F. ; Bernardi, F. D., The calculation of small molecular interactions by the differences of separate total energies. Some procedures with reduced errors. *Mol. Phys.*, **1970**, *19*, 553-566, DOI: 10.1080/00268977000101561.

[27] Reed, A. E.; Curtiss, L. A.; Weinhold, F., Intermolecular interactions from a natural bond orbital, donor-acceptor viewpoint. *Chem. Rev.*, **1988**, *88*, 899-926, DOI: 10.1021/cr00088a005.

[28] a) Glendening, E. D.; Streitwieser, A., Natural energy decomposition analysis: An energy partitioning procedure for molecular interactions with application to weak hydrogen bonding, strong ionic, and moderate donor-acceptor interactions. *J. Chem. Phys.*, **1994**, *100*, 2900-2909, DOI: 10.1063/1.466432; b) Glendening, E. D., Natural energy decomposition analysis: Explicit evaluation of electrostatic and polarization effects with application to aqueous clusters of alkali metal cations and neutrals. *J. Am. Chem. Soc.*, **1996**, *118*, 2473-2482, DOI: 10.1021/ja951834y; c) Schenter, G. K.; Glendening, E. D., Natural energy decomposition Analysis: The Linear Response Electrical Self Energy. *J. Phys. Chem.*, **1996,** *100*, 17152-17156, DOI: 10.1021/jp9612994; d) Glendening, E. D., Natural energy decomposition analysis: Extension to density functional methods and analysis of cooperative effects in water clusters. *J. Phys. Chem. A*, **2005**, *109*, 11936-11940, DOI: 10.1021/jp058209s.

[29] a) Bader, R. F. W., Atoms in molecules. **1985**, *18*, 9-15, 10.1021/ar00109a003; b) Bader, R. F. W., *Atoms in Molecules: A Quantum Theory*. Clarendon Press: 1994.